ORIGINAL ARTICLE

JBMR®

Isl1 Controls Patterning and Mineralization of Enamel in the Continuously Renewing Mouse Incisor

Adrien Naveau,[1,2,3,4]* Bin Zhang,[5,6]* Bo Meng,[1] McGarrett T Sutherland,[1] Michaela Prochazkova,[1,7] Timothy Wen,[1] Pauline Marangoni,[1] Kyle B Jones,[1] Timothy C Cox,[8,9] Bernhard Ganss,[10] Andrew H Jheon,[1] and Ophir D Klein[1,11]

[1]Program in Craniofacial Biology and Department of Orofacial Sciences, UCSF School of Dentistry, University of California, San Francisco, San Francisco, CA, USA
[2]Université Paris Descartes, Sorbonne Paris Cite, UMR S872, Paris, France
[3]Centre de Recherche des Cordeliers, Université Pierre et Marie Curie, UMR S872, Paris, France
[4]INSERM U872, Paris, France
[5]Department of Oral and Maxillofacial Surgery, Guanghua School of Stomatology, Hospital of Stomatology, Sun Yat-Sen University, Guangzhou, Guangdong, China
[6]Guangdong Provincial Key Laboratory of Stomatology, Sun Yat-Sen University, Guangzhou, Guangdong, China
[7]Laboratory of Transgenic Models of Diseases, Institute of Molecular Genetics of the ASCR, v.v.i., Prague, Czech Republic
[8]Department of Pediatrics (Craniofacial Medicine), University of Washington, Seattle, WA, USA
[9]Center for Developmental Biology and Regenerative Medicine, Seattle Children's Research Institute, Seattle, WA, USA
[10]Faculty of Dentistry, University of Toronto, Toronto, ON, Canada
[11]Department of Pediatrics and Institute for Human Genetics, University of California, San Francisco, San Francisco, CA, USA

ABSTRACT

Rodents are characterized by continuously renewing incisors whose growth is fueled by epithelial and mesenchymal stem cells housed in the proximal compartments of the tooth. The epithelial stem cells reside in structures known as the labial (toward the lip) and lingual (toward the tongue) cervical loops (laCL and liCL, respectively). An important feature of the rodent incisor is that enamel, the outer, highly mineralized layer, is asymmetrically distributed, because it is normally generated by the laCL but not the liCL. Here, we show that epithelial-specific deletion of the transcription factor Islet1 (*Isl1*) is sufficient to drive formation of ectopic enamel by the liCL stem cells, and also that it leads to production of altered enamel on the labial surface. Molecular analyses of developing and adult incisors revealed that epithelial deletion of *Isl1* affected multiple, major pathways: Bmp (bone morphogenetic protein), Hh (hedgehog), Fgf (fibroblast growth factor), and Notch signaling were upregulated and associated with liCL-generated ectopic enamel; on the labial side, upregulation of Bmp and Fgf signaling, and downregulation of *Shh* were associated with premature enamel formation. Transcriptome profiling studies identified a suite of differentially regulated genes in developing *Isl1* mutant incisors. Our studies demonstrate that ISL1 plays a central role in proper patterning of stem cell–derived enamel in the incisor and indicate that this factor is an important upstream regulator of signaling pathways during tooth development and renewal. © 2017 American Society for Bone and Mineral Research.

KEY WORDS: TOOTH DEVELOPMENT; MOUSE INCISOR; ECTOPIC ENAMEL; ISL1; AMELOGENESIS

Introduction

Enamel, the outer covering of teeth, is generated from ectoderm-derived epithelial cells, and it is the hardest physiological tissue in vertebrates. The mouse incisor provides a valuable model to study the molecular and cellular mechanisms of enamel formation, or amelogenesis. In the mouse incisor, enamel is normally deposited in an asymmetric fashion exclusively on the labial (toward the lip) surface. This asymmetry is important, because unlike the mouse molar, the incisor renews throughout life in a process that is fueled by mesenchymal and epithelial stem cells.[1] Thus, asymmetric enamel distribution favors abrasion of the softer, enamel-free, lingual (toward the tongue) surface, which maintains proper incisor length and sharpness in light of the continuous growth.

The dental epithelial stem cells (DESCs) responsible for mouse incisor enamel renewal are located in niches called the labial and lingual cervical loops (laCL and liCL, respectively) at the proximal

Received in original form October 28, 2016; revised form June 9, 2017; accepted June 21, 2017. Accepted manuscript online June 26, 2017.
Address correspondence to: Andrew H Jheon, DDS, PhD, Program in Craniofacial Biology and Department of Orofacial Sciences, University of California, San Francisco, 513 Parnassus Avenue, San Francisco, CA 94143, USA. E-mail: andrew.jheon@ucsf.edu
*AN and BZ contributed equally to this work.
Additional Supporting Information may be found in the online version of this article.
Journal of Bone and Mineral Research, Vol. xx, No. xx, Month 2017, pp 1–13
DOI: 10.1002/jbmr.3202

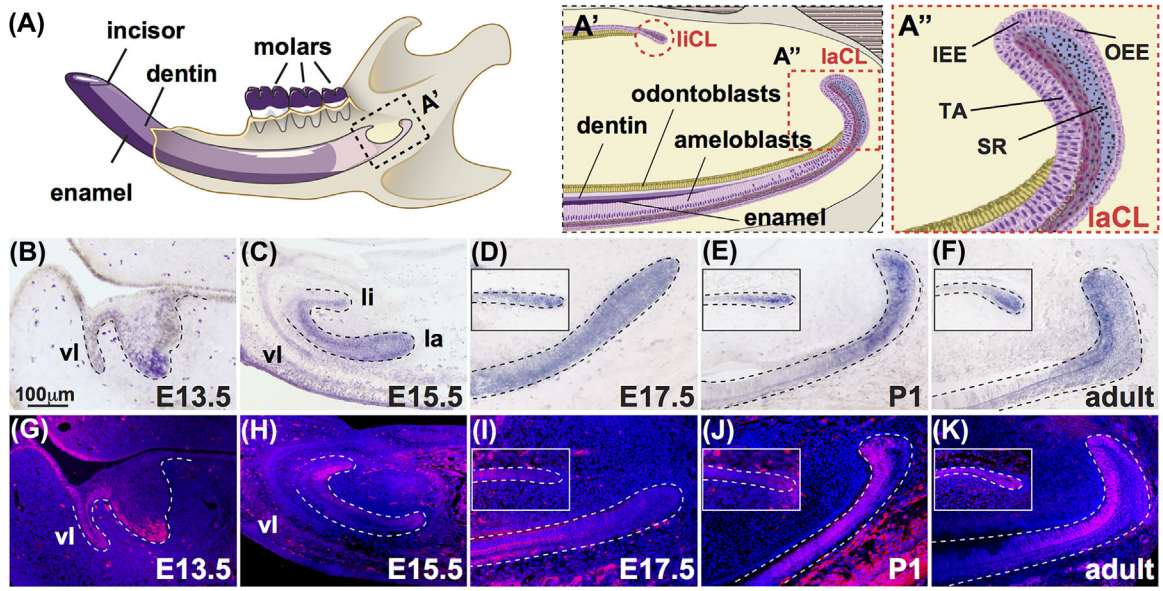

Fig. 1. Expression of *Isl1* during development of the mouse incisor. (*A*) Illustration of the mouse hemimandible showing the incisor and molars, as well as the mineralized dentin and enamel comprising the incisor. (*A'*) The proximal region of the incisor denoting the labial and lingual cervical loop (laCL and liCL, respectively, highlighted by dashed, red lines). (*A''*) Magnified view of the laCL showing the inner enamel epithelium (IEE), outer enamel epithelium (OEE), stellate reticulum (SR), and transit-amplifying cells (T-A). (*B–F*) In situ hybridization staining for *Isl1* at embryonic day 13.5 (E13.5), E15.5, E17.5, postnatal day 1 (P1), and 6 weeks old (adult) showed *Isl1* expression throughout mouse incisor development including the vestibular lamina (vl), and the lingual (li) and labial (la) aspects. In adults, *Isl1* expression was predominant in the laCL and liCL. (*G–K*) Immunofluorescence staining for ISL1 during mouse incisor development showed similar expression profiles to *Isl1* expression (*B–F*) with the exception of E15.5, where protein expression was increased on the lingual side.

end of the incisor (Fig. 1*A*,*A'*).[1–8] The laCL comprises several different cell types including the stellate reticulum (SR), the outer enamel epithelium (OEE), the inner enamel epithelium (IEE), and the transit-amplifying (TA) region, the last of which eventually differentiate into enamel-producing ameloblasts (Fig. 1*A''*).[9] In contrast, the rodent incisor liCL does not normally generate ameloblasts and enamel. Although several studies have focused on the laCL, very little is known about the liCL.

The regulation of ectoderm-derived epithelium during amelogenesis and/or tooth development involves members of the major signaling pathways, including Bmp, Eda, Fgf, Notch, Shh, and Wnt family members.[1,2,10–17] To date, three distinct mouse models have shown that effects on Bmp or Fgf signaling can lead to the generation of ectopic enamel or ameloblasts by the liCL.[15,18,19]

Islet1 (*Isl1*) encodes a LIM-homeodomain (LIM-HD) transcription factor,[20] and mice lacking *Isl1* die at embryonic day (E) 9.5.[21] *Isl1* is involved in many different pathways and processes, including the control of motor neuron and interneuron specification[21] as well as pituitary,[22] pancreas,[23] heart,[24] and hindlimb development.[25] *Isl1* also marks cardiovascular progenitor cells that give rise to cardiomyocyte, smooth muscle, and endothelial cell lineages.[26–30] Recently, *Isl1* was shown to be highly expressed in dental epithelial tumors called ameloblastomas,[31] and was identified in a genomewide association study (GWAS) to potentially play a role in caries development.[32]

Little is known about the function of *Isl1* in tooth development. *Isl1* is expressed in the oral and dental epithelium of the mouse incisor at E10, but its expression is limited to the epithelium in the enamel-free cusp region during molar development.[33] Early embryonic lethality after global deletion of *Isl1* has precluded the study of *Isl1* during tooth development in vivo, but in vitro studies have provided initial insights into the role of ISL1 in tooth patterning, including identification of a positive feedback loop between BMP4 and ISL1.[33] Interestingly, although SHH regulates *Isl1* in neural tissues,[34] in vitro experiments suggested that SHH does not regulate *Isl1* in oral epithelia.[33] Recently, a genomewide gene expression analysis was performed on incisor, canine, and molar germs in 11-week-old human fetuses, and *Isl1* was observed to be expressed in incisor and canine, but not molar, germs.[35]

Here, we generated a conditional null mouse in which *Isl1* was inactivated in epithelial tissue utilizing the *Krt14*^{Cre} driver. *Krt14*^{Cre};*Isl1*$^{fl/fl}$ mice appeared normal and healthy, with the exception of incisor enamel defects, including altered enamel on the labial surface and ectopic enamel on the lingual surface, where enamel is not normally formed. Interestingly, molar teeth were not affected. Multiple signaling pathways, including Bmp, Fgf, Hh, and Notch, were perturbed in the laCL and liCL of control and mutant mice. Thus, *Isl1* appears to play a critical, central role in incisor enamel formation.

Materials and Methods

Animals

All experimental procedures involving mice were approved by the Institutional Animal Care and Use Committee (IACUC) at UCSF and the mice were handled in accordance with the principles and procedure of the Guide for the Care and Use of Laboratory Animals under the approved protocol AN084146-02F. Mice were

maintained in a temperature-controlled facility with access to mouse chow and water ad libitum. Mice carrying the *Krt14*^{Cre} [Tg(KRT14-cre)1Amc][36] and *Isl1*^{fl} [*Isl1*^{tm2Gan}][37] alleles were mated to generate conditional, epithelial-specific, *Isl1*-inactivated mice, namely *Krt14*$^{Cre/+}$;*Isl1*$^{fl/fl}$ and *Isl1*$^{fl/fl}$ mice (referred to as mutants and controls, respectively). To generate age-specific embryos, adult mice were mated overnight and females were checked for a vaginal plug in the morning. The presence of a vaginal plug was designated as embryonic day (E) 0.5. At least three 6-week-old mice were examined at each time point for all experiments unless otherwise specified. Up to five mice of the same sex were housed together until time of sacrifice and no adverse events were reported. Both male and female mice were analyzed.

Histology, in situ hybridization, and immunohistochemistry

Mice were euthanized following standard IACUC protocols. Specimens at E13.5, E15.5, E17.5, postnatal day 1 (P1), and 6 weeks old were collected and fixed overnight in 4% paraformaldehyde at 4°C for 24 to 48 hours, demineralized in 0.5M EDTA for 3 to 14 days if required, dehydrated, embedded in paraffin wax, and serially sectioned at 7 μm. Histological sections were stained with hematoxylin and eosin (H&E). For in situ hybridization analyses, sections were hybridized to digoxigenin (DIG)-labeled RNA probes for detection of RNA transcripts. Sections were treated with 10 μg/mL of proteinase K and acetylated prior to hybridization with probe. DIG-labeled RNA probes were synthesized from plasmids containing full-length cDNA or fragments of *Isl1*, *Shh*, *Fst*, *Etv5*, *Fgf9*, *Fgf10*, *Spry2*, and *Bmp4*. Immunohistochemistry was performed according to standard protocols. Antigen retrieval was performed by boiling the slides in Trilogy (Cell Marque, Rocklin, CA) for 15 min and cooled at room temperature for 20 min after removing paraffin and rehydration. Primary antibodies used were as follows: anti-ISL1 (1:200; ab20670; Abcam, Cambridge, MA, USA), anti-AMEL (amelogenin; 1:200; Abcam), anti-AMBN (ameloblastin; 1:200; Abcam), anti-CLDN1 (Claudin1; 1:200; Abcam), anti-NICD (Cleaved Notch1 (Val1744); 1:200; Cell Signaling Technology, Beverly, MA, USA). Goat anti-rabbit or mouse AlexaFluor 555 secondary antibodies were used (1:500; Invitrogen, Carlsbad, CA, USA).

Detection of proliferating cells

Proliferating cells were identified by injection of 1 mg BrdU for 90 min followed by staining with a rat monoclonal anti-BrdU antibody (1:1000; Abcam). Slides were treated with 0.2N HCl prior to applying antibody, and BrdU-positive cells were visualized using a goat anti-rat AlexaFluor 555 secondary antibody (1:500; Invitrogen).

Microscopy

Fluorescent and bright-field images were taken using a DM5000B microscope with a DFC500 camera (Leica, Wetzlar, Germany). For confocal images, an SP5 Upright Confocal microscope (Leica) was used.

Micro–computed tomography

Micro–computed tomography (μCT) was performed on a MicroXCT-200 (Xradia, Pleasanton, CA, USA) through the MicroCT Imaging Facility at UCSF. Each specimen was scanned at 75 KVp and 6W at magnification ×4. Specimens were also imaged at the Small Animal Tomographic Analysis (SANTA) facility located at the Seattle Children's Research Institute using a Skyscan 1076 micro-Computed Tomograph (Skyscan, Aartselaar, Belgium). Scans were done at an isotropic resolution of 17.21 μm using the following settings: 55 kV, 179 μA, 0.5 mm aluminum filter, 460 ms exposure, rotation step of 0.7 degrees, 180-degree scan, and 3 frame averaging. All data were reconstructed using Nrecon (v1.6.9.4) with the same grayscale threshold. Reconstructions were all converted to 3D volumes using Drishti v2.4 (http://anusf.anu.edu.au/Vizlab/drishti/).

RNA isolation, qPCR, and RNA-Seq

Total RNA was isolated using the RNeasy kit (Qiagen, Valencia, CA, USA). DNA was removed in-column with RNase-free DNAse (Qiagen). All qPCR reactions were performed using the GoTaq qPCR Master Mix (Promega, San Luis Obispo, CA, USA) in a Mastercycler Realplex (Eppendorf, Hamburg, Germany). Prime-Time Primers (Integrated DNA Technologies [IDT], Coralville, IA, USA) were utilized for qPCR and primer sequences are available upon request. qPCR conditions were as follows: 95°C, 2 min; 40 cycles at 95°C, 15 s; 58°C,15 s; 68°C, 20 s; followed by a melting curve gradient. Expression levels of the genes of interest were normalized to levels of *Rpl19*.

For RNA-Seq experiments, *Krt14*$^{Cre/+}$;*Isl1*$^{fl/fl}$ mice were mated with RFP mice to generate *Isl1*$^{fl/fl}$;RFP (control) or *Krt14*$^{Cre/+}$;*Isl1*$^{fl/fl}$;RFP (mutant) mice. Developing incisors from E15.5 embryos were dissected and total RNA isolated as described in the previous paragraph. RNA-Seq experiments were performed at the SABRE Functional Genomics Core at UCSF (http://arrays.ucsf.edu/). Briefly, total RNA quality was assessed by spectrophotometry (NanoDrop; Thermo Fisher Scientific Inc., Rockford, IL, USA) and Agilent 2100 Bioanalyzer (Agilent Technologies, Santa Clara, CA, USA). RNA sequencing libraries were generated using the TruSeq stranded mRNA sample prep kits with multiplexing primers, according to the manufacturer's protocol (Illumina, San Diego, CA, USA), and library concentrations were measured using KAPA Library Quantification Kits (Kapa Biosystems, Inc.). Equal amounts of indexed libraries were pooled and sequenced on the Illumina HiSeq 2500 (Illumina). Data analysis involved demultiplexing the results, trimming adapter sequences from the reads, and aligning unique reads to the mouse genome (mm10). Sequence alignment and splice junction estimation were performed using software programs Bowtie2 (http://bowtie-bio.sourceforge.net/bowtie2/index.shtml)[38] and TopHat (http://ccb.jhu.edu/software/tophat/index.shtml),[39] respectively. For differential expression testing, the genomic alignments were restricted to those mapping to an annotated transcriptome provided by Ensembl.[40] This subset of mappings was aggregated on a per-gene basis as raw input for the program DESeq.[41]

Gene ontology (GO) analysis was performed using the Database for Annotation, Visualization and Integrated Discovery (DAVID Bioinformatics Resource v6.7; available at https://david-d.ncifcrf.gov).[42,43] Enriched GO terms for Biological Processes were detected and clustered using the default parameters for Functional Annotation Clustering. Annotation Clusters displaying an Enrichment Score of 1.3 and above were listed (Supporting Fig. S6). GO analysis was focused on genes differentially expressed by twofold or higher (upregulation or downregulation) with a false discovery rate (FDR) less than 0.01. Of 139 downregulated entries, 22 were not referenced in the DAVID platform, whereas 12 of 131 upregulated entries were not referenced.

Scanning electron microscopy

Mouse hemimandibles were dissected free of soft and connective tissue, fixed in 4% PFA in PBS overnight, then dehydrated in a graded ethanol series and dried in a vacuum desiccator. Hemimandibles were then embedded in epoxy resin (resin 105 and hardener 205 at a ratio of 5:1 wt/wt; WestSystem, Bay City, MI, USA), ground to the desired thickness on a plate grinder (EXAKT 400CS; EXAKT Advanced Technologies GmbH, Norderstedt, Germany) using 800 grit silicon carbide paper and polished with 2000 and 4000 grit silicon carbide paper (Hermes Abrasives, Mississauga, ON, Canada). The exposed tissue was etched with 10% phosphoric acid for 30 s, rinsed with water, and dried in a vacuum desiccator. Samples were mounted on scanning electron microscopy (SEM) stubs with carbon tape, surfaces coated with 7 nm gold using a sputter coating machine (Desk II; Denton Vacuum, Moorestown, NJ, USA), and imaged in a Philips SEM instrument (XL30 ESEM; Philips, Andover, MA, USA) operating at a beam energy of 20 keV in secondary electron or backscatter mode. Images were processed using Adobe Photoshop CS5.1 (Adobe, San Jose, CA, USA) to adjust upper and lower limits of input levels in grayscale mode, and to apply autobalance and autocontrast settings. Please refer to Supporting Methods for analysis of structure and relative mineral density of enamel using SEM.

Statistical analysis

All experiments were performed independently at least three times (ie, $n = 3$) in triplicates, and when applicable, presented as an average $\pm$ SE. Student's *t* test was used to determine *p* values; $p < 0.05$ was deemed to be significant.

Results

Isl1 is expressed in the dental epithelium during development of the mouse mandibular incisor

We first analyzed the expression of *Isl1* during mouse tooth development by in situ hybridization and immunofluorescence staining (Fig. 1*B–K*). *Isl1* mRNA and protein were detected predominantly in the developing mandibular incisor (Fig. 1*B–E*, *G–J*) with little or no expression in molars (Supporting Fig. S1). At E13.5, *Isl1* was expressed in the dental epithelium, vestibular lamina (vl), and the labial aspect of the incisor tooth bud (Fig. 1*B*,*G*). At E15.5, *Isl1* expression was diminished in the dental epithelium and vl, but was observed on both the lingual (li) and labial (la) sides of the developing incisor (Fig. 1*C*,*H*). Interestingly, ISL1 protein appeared increased on the lingual aspect (Fig. 1*H*). At E17.5 and P1, *Isl1* expression was restricted to the proximal regions of the incisor, namely the liCL and laCL (Fig. 1*D*,*E*,*I*,*J*). Last, in adult (ie, 6 weeks old), mandibular incisors *Isl1* expression was predominantly observed in the IEE, TA, and preameloblast region of the laCL, whereas in the liCL, expression was limited to the most proximal region (Fig. 1*F*, *K*). We observed similar expression patterns in adult maxillary incisors (data not shown).

Conditional inactivation of epithelial *Isl1* leads to incisor defects

Global inactivation of *Isl1* causes early embryonic lethality.[21] Because *Isl1* is predominantly expressed in dental epithelia (Fig. 1*B–K*), we generated mice carrying an epithelial-specific deletion of *Isl1*. Adult $Krt14^{Cre}$;$Isl1^{fl/fl}$ mutant mice were viable and appeared healthy overall, but all mutant mice possessed white incisors with blunted tips, as compared to the yellow, sharp incisors in controls (Fig. 2*A*,*E*,*M*). We also observed a diastema or space, between the maxillary incisors in 30% to 50% of the mutants (Fig. 2*B*,*C*,*F*,*G*,*M*), and the bony socket housing the maxillary incisors appeared to be enlarged in mutants compared to controls (Fig. 2*C*,*G*).

We next examined the mineralized tissues in the mutants by μCT analysis of the mandibular incisors and found two distinct phenotypes. First, ectopic enamel was present on the lingual incisor surface in mutants both in sagittal (Fig. 2*D*,*H*) and cross-section (Fig. 2*D*′,*H*′) with 100% penetrance (Fig. 2*M*). Second, enamel mineralization occurred prematurely or closer to the laCL in mutants (Fig. 2*D*,*H*). The μCT results were confirmed histologically in P1 mice (Fig. 2*I–L*″). Incisor enamel matrix was observed on the lingual surface of the mutant but not control mandibular incisor in cross-sectional (Fig. 2*I–I*″,*K–K*″) and sagittal view (Fig. 2*J–J*″,*L–L*″). Moreover, premature enamel mineralization as indicated by the presence of enamel matrix was also confirmed histologically (Fig. 2*J*,*L*). In contrast to the incisors, we did not detect any differences in mutant molars using μCT (Supporting Fig. S2A,B) or SEM (Supporting Fig. S2C,D) analyses.

Deletion of *Isl1* leads to altered labial enamel and enamel-like mineralized tissue on the lingual surface

SEM analyses of control and mutant hemimandibles in sagittal view revealed defects in labial enamel (Fig. 3*A–D*[3]). In control incisors, the enamel rods extend from the dentinoenamel junction (DEJ) to near the surface (Fig. 3*B*). In mutants, enamel rods appeared normal near the DEJ (Fig. 3*D*,*D*[1]) but became disorganized and lost their distinctive enamel rod pattern approximately halfway between the DEJ and surface (Fig. 3*D–D*[3]). In addition, the lingual surface in mutants had enamel-like mineralization, with moderately organized enamel-like rods extending from the DEJ to the surface (Fig. 3*E*).

Interestingly, we could not detect differences in incisor labial enamel density using μCT (Supporting Fig. S2E,F) and SEM backscatter (Supporting Fig. S2G-J) analyses. The density of the ectopic lingual incisor enamel was also similar to labial enamel (Supporting Fig. S2E). In mutant labial enamel, the outer layer or approximately one-third of the enamel on the surface or at the side facing the embedding resin, appeared more uniform and highly mineralized than wild-type specimens (Supporting Fig. S2G,H). This increased uniformity of mutant enamel was reflected in the narrower peak width of the enamel signal (grayscale value of ~200) in the corresponding histograms (Supporting Fig. S2I,J), whereas the number of pixels of the mutant enamel peak was ~8000) compared to the control enamel peak of ~4000 was indicative of more densely mineralized enamel (Supporting Fig. S2I,J). However, mutant enamel showed a higher but narrower peak compared to the lower but broader peak in controls suggesting overall enamel densities may be similar. Moreover, we did not detect any differences in labial enamel volume or thickness when the mandibular incisor was analyzed between the distal incisor tip and first molar distal root to control for premature enamel mineralization in mutants (data not shown). Additional experiments are required to further analyze control and mutant incisor enamel but it is interesting that "white" enamel did not indicate hypomineralized enamel.

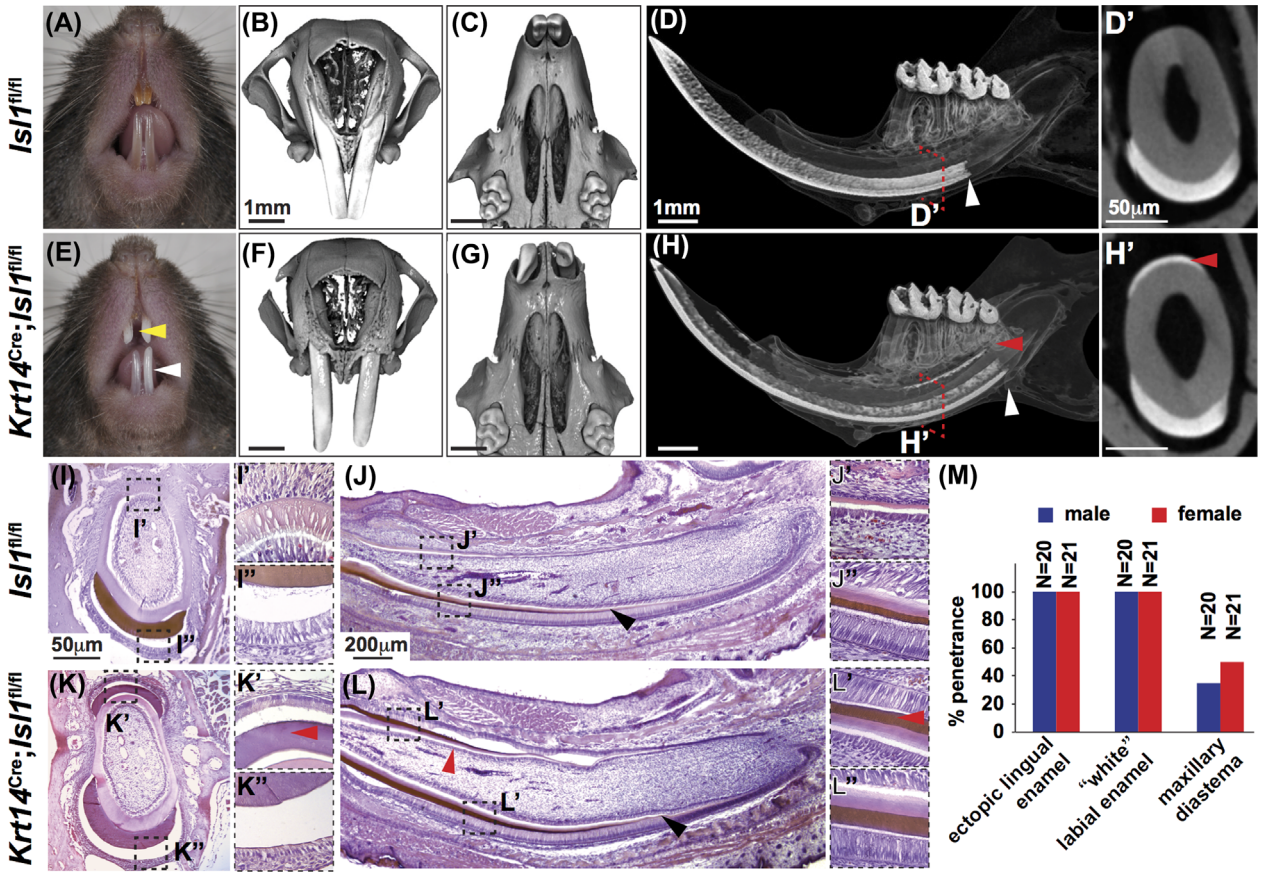

Fig. 2. Conditional inactivation of *Isl1* in mouse epithelia leads to mice with enamel defects. (*A–H'*) Comparison of control (*Isl1*$^{fl/fl}$) and conditionally inactivated (*Krt14*^{Cre};*Isl1*$^{fl/fl}$) adult mouse incisors. Control mice exhibited shiny, yellow shading of maxillary and mandibular incisors (*A*; white arrowheads), whereas mutant mice showed white enamel (*E*; white arrowheads). μCT analyses of maxillae in frontal (*B,F*) and ventral (*C,G*) view showed a diastema between the incisors in mutant (*F,G*) but not control (*B,C*) mice with enlarged tooth sockets in mutant mice (*G*; red arrowhead). μCT analyses of the hemimandible in sagittal view (*D,H*) and the incisor in cross-section (*D',H'*) demonstrated the presence of ectopic enamel on the lingual surface (yellow arrowheads) where enamel is normally absent (*D,D'*). Furthermore, enamel appeared to be generated prematurely in mutant mice compared to controls (*D,H*; white arrowheads). (*I–L''*) Hematoxylin and eosin staining of P0 hemimandible in cross-section (*I–I'',K–K''*) and sagittal view (*J–J'',L–L''*) showed ectopic enamel matrix on the lingual side of mutant (*K–K''*, *L,L'*; red arrowheads) but not control (*I–I'',J,J'*) incisors. Enamel and dentin matrix appeared normal in mutants (*L,L''*) compared to controls (*J,J''*); however, enamel was generated prematurely in mutants (*L*; black arrowhead) compared to controls (*J*; black arrowhead). (*M*) There was 100% penetrance of the ectopic, lingual enamel and white labial enamel phenotypes. The maxillary diastema was observed in less than one-half of the mutants.

Abnormalities in enamel mineralization and ameloblast differentiation were also evidenced by immunofluorescence staining for two ameloblast markers, amelogenin (AMEL) and ameloblastin (AMBN) (Fig. 3*F–M*). AMEL and AMBN were detected in the mutant liCL (Fig. 3*G,K*), reflecting the ectopic enamel formation, in contrast to the control (Fig. 3*F,J*). In the laCL, both AMEL and AMBN were present in controls and mutants, but expression of both markers occurred earlier in mutants (Fig. 3*H,I,L–O*). Additional enamel proteins including enamelin (ENAM), kallikrein-4 (KLK4), and amelotin (AMTN) were assayed and shown to be expressed in the lingual aspect of the mutant incisor further supporting the generation of ectopic enamel or enamel-like tissue (Supporting Fig. S3A,B,E,F,I,J). Moreover, ENAM and KLK4 appeared to be prematurely expressed (Supporting Fig. S3C,D,G,H,M) similar to AMEL and AMBN. Interestingly, AMTN did not show premature, mutant expression (Supporting Fig. S3K-M).

The ectopic and premature expression of enamel proteins (eg, AMEL, AMBN, AMTN, ENAM, and KLK4) in adult liCL and laCL suggested a change in the number of proliferative cells (Fig. 4). Indeed, we observed an increased number of proliferating cells in the mutant liCL, although there was no change in the size of the zone of BrdU+ cells (Fig. 4*A–D*). Conversely, we observed a decrease in the number of proliferative cells in the laCL of mutants, as well as a shortened zone of BrdU+ cells (Fig. 4*E–H*).

Epithelial-specific deletion of *Isl1* affects multiple signaling pathways

Shh is an important regulator of the ability of dental epithelial stem cells to generate ameloblast progenitors in the laCL.[3] In adult incisors, we found differences in *Shh* expression in both the liCL (Fig. 5*A–C*) and laCL (Fig. 5*J–L*) using both in situ

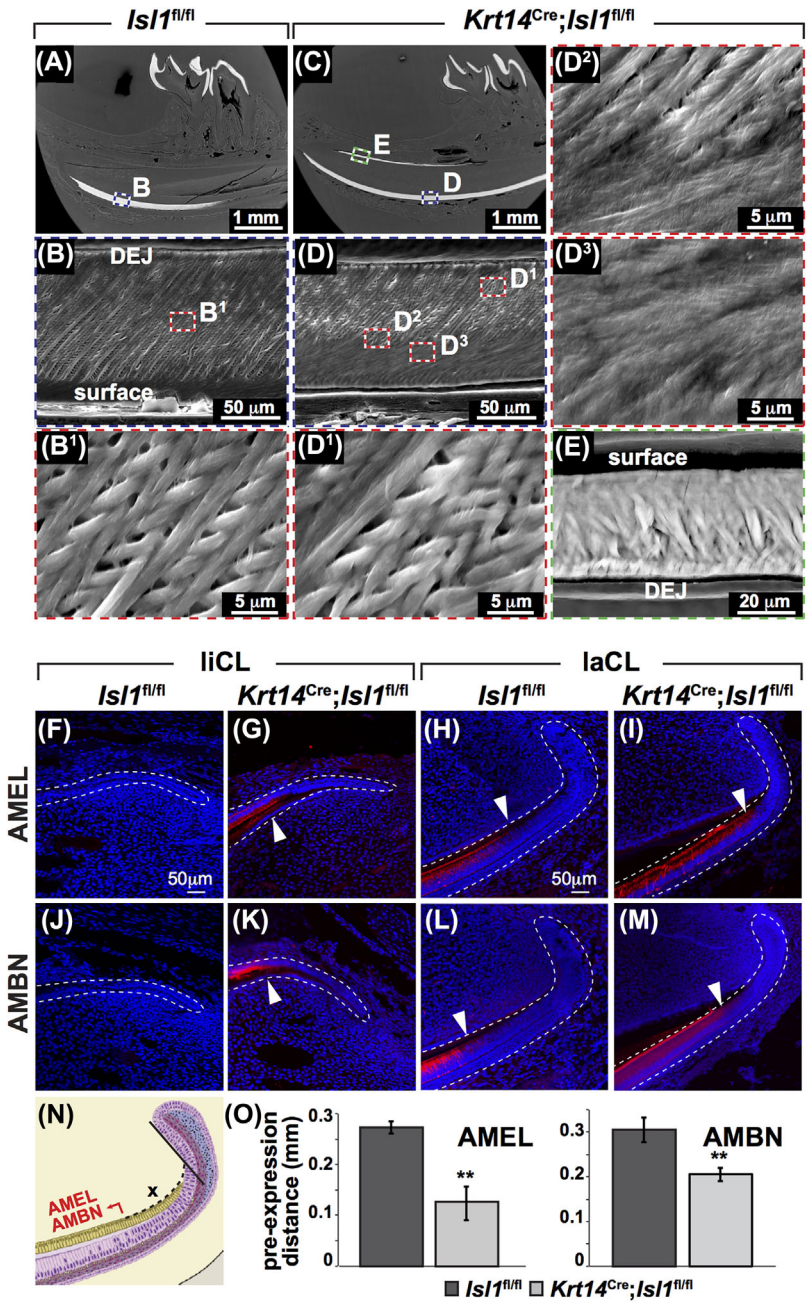

Fig. 3. Conditional epithelial inactivation of mouse *Isl1* leads to defects in enamel mineralization. (*A–E*) Scanning electron microscopy (SEM) of the hemimandible in sagittal view of control (*A–B*^{1}) and mutant (*C–E*) mice. Control enamel (*B*,*B*^{1}) showed parallel enamel rods that ran continuously from the dentin-enamel junction (DEJ) to the surface with a 45-degree distal orientation. In mutants, the inner enamel (ie, enamel near the DEJ) showed a similar pattern compared to controls (*B*^{1},*D*^{1}); however, this pattern was lost approximately halfway between the DEJ and the surface (*D*^{2},*D*^{3}). Ectopic lingual enamel showed enamel-like mineralization (*E*). (*F–O*) Amelogenin (AMEL) and ameloblastin (AMBN) showed ectopic and premature expression in mutant liCL and laCL, respectively. AMEL and AMBN are normally not expressed in the liCL (*F*,*J*) but was expressed in mutant liCL (*G*,*K*). AMEL and AMBN were expressed in the laCL of control and mutant incisors; however, they were expressed prematurely (*H*,*I*,*L*,*M*; white arrowheads). (*N*,*O*) The premature expression of AMEL and AMBN was quantified and confirmed. $^{**}p < 0.01$. AMBN = ameloblastin; AMEL = amelogenin; DEJ = dentin-enamel junction; SEM = scanning electron microscopy.

hybridization and qPCR. Interestingly, *Shh* expression was increased in the liCL, whereas it was decreased in the laCL, demonstrating that ISL1 functions in a context-dependent fashion. Moreover, in the mutant liCL, *Etv5*, a readout of Fgf signaling,[44,45] and *Fst*, an antagonist of Bmp signaling[46,47] were upregulated and downregulated, respectively (Fig. 5*D–I*). On the labial side, *Etv5* expression showed no difference between control and mutant laCL, whereas *Fst* expression was decreased in mutant laCL (Fig. 5*M–R*).

We further analyzed genes in the Fgf and Bmp signaling pathways using in situ hybridization (Supporting Fig. S4). Sprouty2 (*Spry2*), a gene encoding an intracellular antagonist of

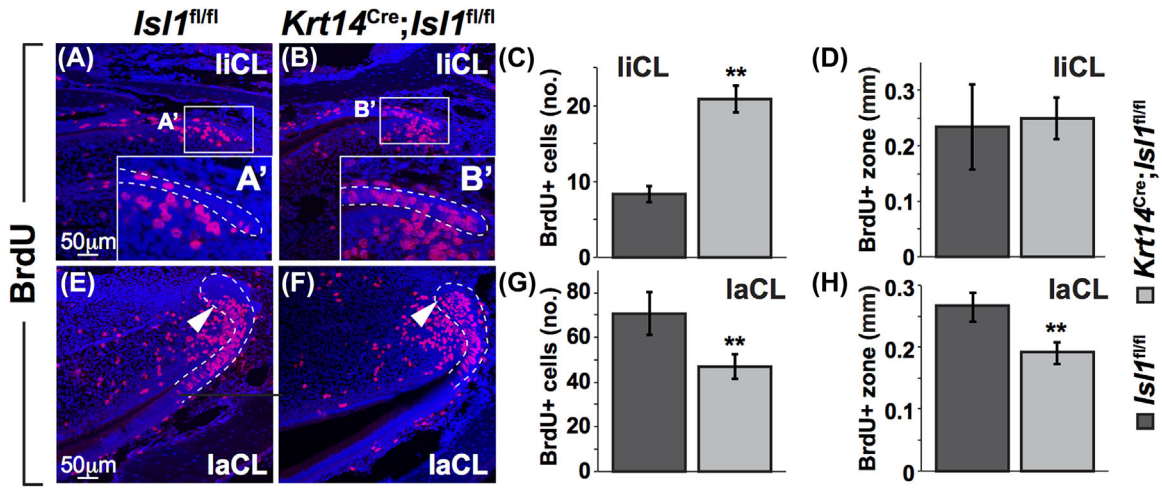

Fig. 4. Conditional epithelial inactivation of *Isl1* leads to effects on proliferation in the liCL and laCL of mandibular mouse incisors. (*A–H*) BrdU was injected for 90 min to label proliferating cells in the liCL and laCL (denoted by white, dashed lines). Magnified view of the liCL (*A'*,*B'*) showed an increase in the number of proliferating cells in mutants (*B'*) compared to controls (*A'*). The number of BrdU+ cells was quantified and confirmed to be increased in mutants (*C*); however, the length of the BrdU+ zone was unchanged. Conversely, in the laCL, the number of BrdU+ cells was quantified and shown to be decreased in mutants compared to controls (*E–G*). Furthermore, the length of the BrdU+ zone was significantly shortened in mutants (*H*). $^{**}p < 0.01$.

Fgf signaling, appeared to be downregulated in the mutant liCL (Supporting Fig. S4A,B), consistent with the upregulation of *Etv5* we observed in the mutant liCL (Fig. 5*D–F*). In the mutant laCL, there appeared to be no or little difference in *Spry2* expression compared to controls (Supporting Fig. S4C,D). No obvious differences in *Fgf9* and *Fgf10* expression were observed in control and mutant liCL and laCL (Supporting Fig. S1E-L). Finally, *Bmp4* expression appeared to be increased in the mutant liCL and laCL (Supporting Fig. S4M-P), which correlated with a decrease in *Fst* expression (Fig. 5*P–R*).

Immunofluorescence staining showed changes in expression of several key proteins between control and mutant liCL and laCL (Fig. 6). pMEK was upregulated in mutant liCL and laCL compared to controls (Fig. 6*A–D*). Moreover, pMEK localization was altered in mutant laCL, with increased staining in the TA and preameloblast regions (white arrowhead) and decreased staining in the OEE (yellow arrowhead; Fig. 6*C*,*D*). pSMAD1/5/8 was also upregulated in mutant liCL and laCL (Fig. 6*E–H*). NICD or activated/cleaved NOTCH1 was upregulated in mutant liCL, but no difference was noted in the laCL (Fig. 6*I–L*). Claudin1 (CLDN1), a tight junction component of epithelial polarized cells[48] that is potentially involved in mouse incisor[49] and human tooth development,[50] appeared to be increased in mutant liCL, but no difference was noted in control and mutant laCL (Fig. 6*M–P*).

Because NICD1, CLDN1, and *Shh* demonstrated differential expression in adult control and mutant incisors, we further assayed their expression during development (Fig. 7). Expression of NICD showed no differences between control and mutant incisors at E14.5, E15.5, and E17.5 (Fig. 7*A–C*,*E–G*). At P1, an important difference was observed, as NICD expression was maintained in the mutant but not control liCL (Fig. 7*D*,*H*) and this NICD expression persisted in adult mutant liCL (Fig. 6*I*,*J*). Expression of CLDN1 protein was similar in developing incisors at E14.5 and E15.5 in controls and mutants, but at E17.5 maintenance of intense CLDN1 expression was observed in mutant liCL (Fig. 7*I–N*), consistent with the strong CLDN1 expression in adult mutant liCL (Fig. 6*M*,*N*). Last, *Shh* expression was assayed during incisor development (Fig. 7*O–T*). Differences in expression patterns were first evident at E15.5, with *Shh* expression noted on the lingual side of the developing mutant incisor (Fig. 7*P*,*S*). This expression pattern was maintained in mutant incisors at E17.5 (Fig. 7*Q*,*T*), at P1 (data not shown), and in adults (Fig. 5*A–C*,*J–L*).

RNA-Seq analysis points to numerous differentially expressed genes in control and mutant E15.5 mandibular incisors

In light of the myriad effects of *Isl1* deletion on signaling pathways, we next took an unbiased approach to determine the effects of *Isl1* deletion on gene expression. We analyzed the transcriptome of cells from developing incisors at E15.5 because this was the earliest stage at which we noted a difference in gene expression between control and mutant mice (Fig. 7*O–T*). RNA-Sequencing (Seq) analysis revealed 131 genes that were differentially expressed by twofold or higher (ie, $\log_2$ fold change [FC] relative to the global average for differentially expressed genes) with a FDR less than 0.01 (ie, FDR < 0.01) (Fig. 8*A*; Supporting Fig. S5). The control and mutant groups clustered convincingly in our principal component analysis (PCA; Supporting Fig. S6A). From a list of all differentially expressed genes with an FDR < 0.01, we focused on 10 genes for confirmation based on previous known associations with ISL1, involvement in craniofacial development, and/or known expression in developing teeth at approximately E15.5 (Fig. 8*B*). Using qPCR, we confirmed that six of these 10 genes were indeed significantly differentially expressed. *Otx1* and *Tekt2* play a role in inner ear development[51,52]; *Scg2* (also known as secretoneurin) interacts with STAT3, a known ISL1-interaction partner[53,54]; *Ptprv* is associated with bone and energy metabolism,[55] as well as P53-induced cell cycle exit[56];

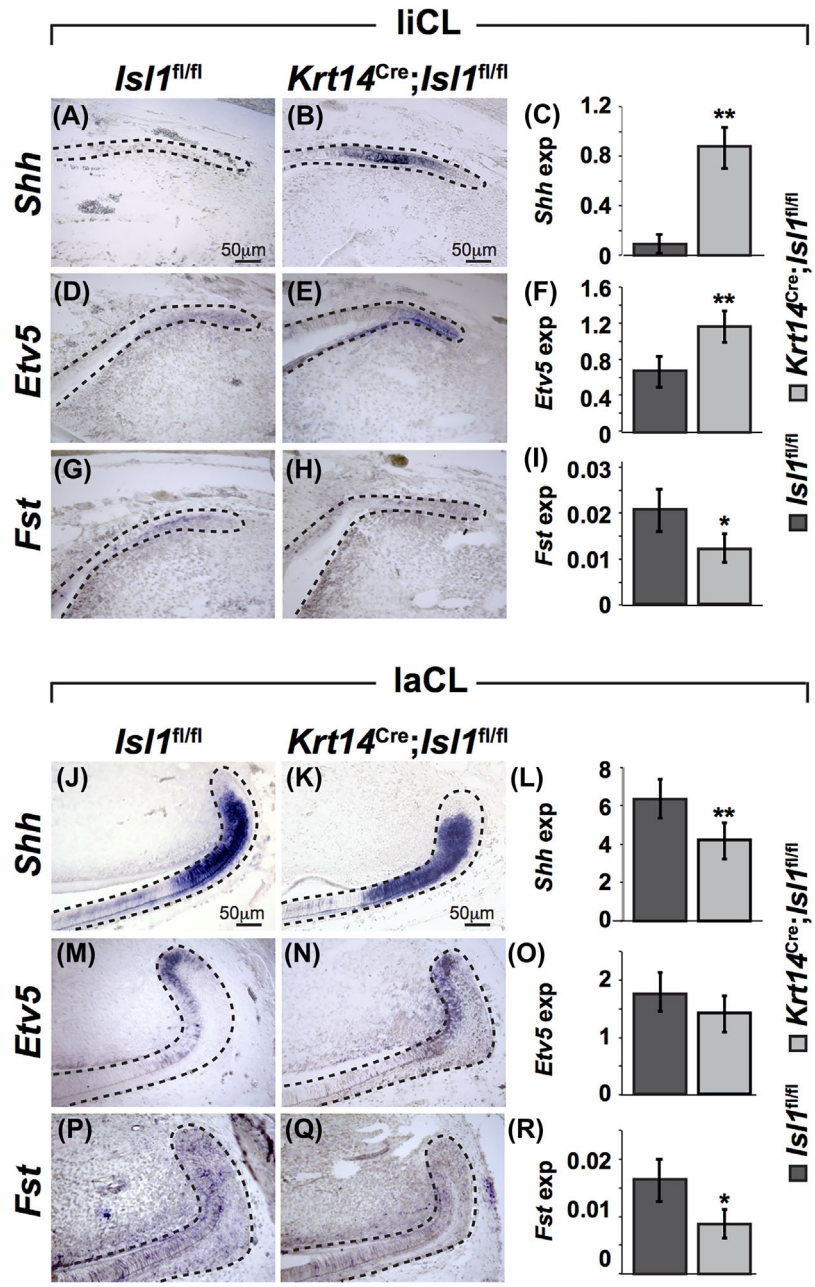

Fig. 5. Differential expression of genes from various signaling pathways in control and mutant mandibular incisors. (*A–I*) Genes from various signaling pathways were analyzed by in situ hybridization and qPCR in the liCL. Expression of *Shh* and *Etv5* was increased in mutant liCL (*B*,*E*) compared to controls (*A*,*D*), whereas *Fst* was decreased in mutant liCL (*H*) compared to controls (*G*). The in situ hybridization results were confirmed by qPCR analyses (*C*,*F*,*I*). (*J–R*) Genes from various signaling pathways were analyzed by in situ hybridization and qPCR in the laCL. Expression of *Shh* and *Fst* expression was decreased in mutants (*J–L*, *P–R*), and *Etv5* showed no difference in expression between control and mutants (*M–O*). $^{*}p < 0.05$; $^{**}p < 0.01$.

Pdzk1ip1 (or *Pdzk1*-interacting protein 1) also interacts with Twist1, an important regulator of the Bmp signaling pathways[57]; and *Stfa1* was observed to be overexpressed in a mouse psoriasis model.[58] Moreover, *Otx1*, *Ptprv*, and *Scg2* are all expressed in E14.5 incisor tooth germs (http://genepaint.org/Frameset.html). The remaining four genes, *Kif27a*, *Frem3*, *Shisa7*, and *Hmgn2*, showed similar trends to the RNA-Seq results but did not reach statistical significance (Fig. 8*B*,*C*).

GO analysis was conducted on genes differentially expressed by twofold or higher (upregulation or downregulation) with an FDR <0.01. This represents 139 downregulated and 131 upregulated genes. GO for our dataset consisted of 14 annotation clusters for the downregulated entries (with two clusters displaying an enrichment score higher than 1.3), and 45 annotation clusters for the upregulated entries (with 12 clusters displaying an enrichment score higher than 1.3). The GO

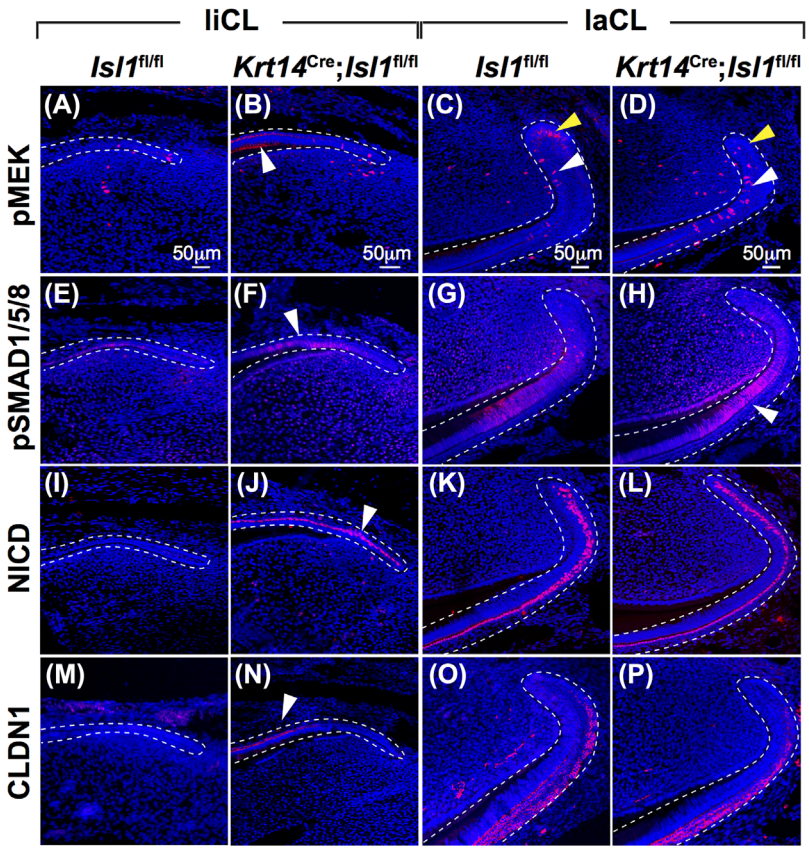

Fig. 6. Differential expression of proteins from various signaling pathways in control and mutant mandibular incisors. (*A–P*) Immunofluorescence staining showed differential expression of numerous proteins in the liCL and laCL regions. pMEK (*A,B*), pSMAD (*E,F*), NICD (*I,J*), and CLDN1 (*M,N*) were all upregulated in mutant liCL (white arrowheads). In the laCL, only pMEK (*C,D*) and pSMAD (*G,H*) appeared to be upregulated in mutants; NICD (*K,L*) and CLDN1 (*O,P*) remained unchanged.

terms demonstrated that a diverse set of processes was impacted in the mutant (Supporting Fig. S6).

Discussion

Amelogenesis is a complex process that involves multiple signaling pathways. In the mouse incisor, enamel is generated on the labial surface (or crown-analog) by DESCs housed in the laCL. After proliferation in the TA region, the DESC progeny differentiate into enamel matrix-secreting ameloblasts. However, relatively little is known about the liCL, which normally does not make enamel on the lingual incisor surface (or the root-analog). Epithelial-specific deletion of *Isl1* in *Krt14*^{Cre};*Isl1*$^{fl/fl}$ mutants resulted in incisors with altered enamel on the labial side and ectopic enamel-like tissue on the lingual side. Analyses of mouse models allow us to further dissect the cellular and molecular mechanisms of amelogenesis, which is potentially relevant to human tooth development.

Ectopic lingual enamel or ameloblasts have only been observed in three other genetically modified mice, all of which pointed to a central role for FGF and BMP signaling in the maintenance of asymmetric incisor enamel (ie, enamel present only on the labial surface). First, alterations in Bmp signaling via inactivation of the extracellular antagonist follistatin (*Fst*) led to the presence of ectopic, lingual ameloblast-like cells.[15] *Fst* is normally expressed in the liCL (Fig. 5*G*), and its inactivation led to the expression of ectopic mesenchymal FGF3.[15] Because *Fst*-null mice exhibited perinatal lethality, the adult phenotype in these mice could not be studied. Second, the combined inactivation of the intracellular FGF antagonists *Spry2* and *Spry4* (*Spry2*$^{+/-}$;*Spry4*$^{-/-}$ mice) resulted in ectopic lingual enamel production.[18] Ectopic mesenchymal *Fgf3* and *Fgf10* expression was detected in these mice near the liCL, and this was correlated with the differentiation of liCL-generated ameloblasts.[18] Third, deletion of the transcriptional repressor, *Ctip2*/*Bcl11b*, resulted in the inversion of *Fgf3* and *Fgf10* expression patterns.[19] This observation was correlated with a decrease in the size of the laCL along with abnormal ameloblasts, whereas the liCL was expanded in association with the generation of ameloblast-like cells.[19] However, similar to *Fst*-null mice, *Bcl11b*-null mice were perinatal lethal, which hindered comprehensive study of the cellular and molecular mechanisms of mutant incisors. Thus, our findings are distinct from the three prior mutants presenting with ectopic lingual enamel in that ISL1 is the first transcription factor to be identified whose conditional inactivation led to ectopic lingual enamel in viable and healthy mice.

Epithelial *Isl1* inactivation resulted in alterations of all the major pathways that we tested, including the Bmp, Hh, Fgf, and Notch signaling pathways. The changes in the Bmp and

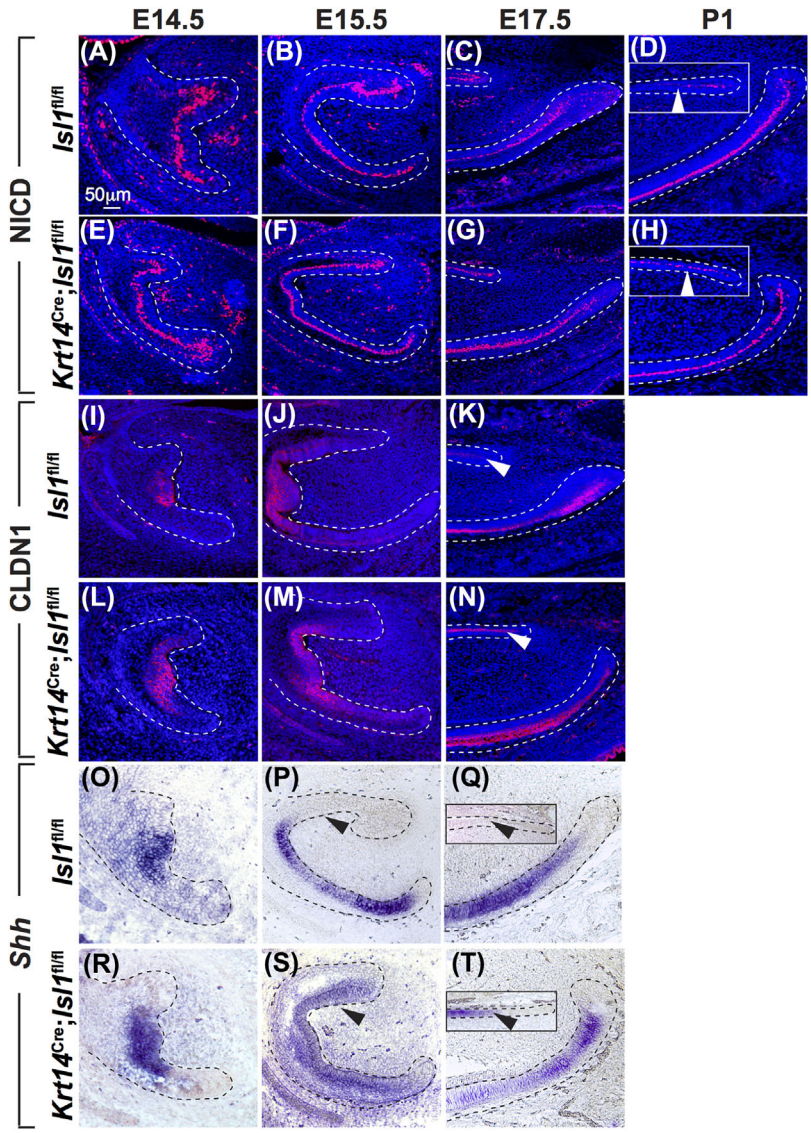

Fig. 7. Expression of NICD, CLDN1, and *Shh* in the CLs during development. (*A–H*) Immunofluorescence staining for NICD showed similar patterns of expression in control and mutant mandibular incisors until E17.5 (*C,G*). At P1, NICD staining decreased in control liCL but remained in the mutant liCL (*D,H* insets; white arrowheads). There appeared to be little difference in NICD expression between control and mutant laCL. (*I–N*) Immunofluorescence staining for CLDN1 showed similar patterns of expression in the enamel knot area until E15.5 (*I,J,L,M*). However, similar to NICD staining at P1 (*D,H* insets), CLDN1 staining remained high in the mutant liCL but decreased in control liCL (*K,N*; white arrowheads). Again, there appeared to be little difference in CLDN1 expression in control and mutant laCL. (*O–T*) In situ hybridization analyses showed similar expression patterns in control and mutant mandibular incisors at E14.5 (*O,R*). At E15.5, *Shh* expression was evidenced on the lingual aspect of the mutant incisors but not in controls (*P,S*). At E17.5, *Shh* expression was present in mutant but not control liCL (*Q,T* insets; black arrowheads). At E17.5, consistent with observations in adult laCL (Fig. 5*J–L*), there appeared to be decreased expression in mutant laCL compared to controls (*Q,T*).

Fgf signaling pathways were consistent with previous reports.[15,18,19] In the mutant liCL, Fgf signaling was increased, as evidenced by the upregulation of *Etv5* (Fig. 5*D–F*) and pMEK (Fig. 6*A,B*) and downregulation of the intracellular Fgf antagonist *Spry2* (Supporting Fig. S4A,B). Bmp signaling was also hyperactivated in mutant liCL, as demonstrated by the upregulation of *Bmp4* (Supporting Fig. S4M,N) and pSMAD1/5/8 (Fig. 6*E,F*), and the downregulation of the Bmp antagonist *Fst* (Fig. 5*G–I*). NICD or NOTCH1 intracellular domain was expressed in mutant adult liCL (Fig. 6*I,J*), which appeared to be due to the retention of NICD expression in the liCL (Fig. 7*A–H*). The differences in NICD expression suggest a disruption in signaling between ameloblasts and the underlying stratum intermedium (SI).[59,60] *Shh* expression was also maintained in the mutant liCL (Fig. 5*A–C*). Differences in *Shh* expression were first detected at E15.5 (Fig. 7*O–T*), and SHH has been shown to regulate DESCs during differentiation of ameloblast progenitors in the laCL.[3] In summary, the epithelial deletion of *Isl1* led to increased signaling through at least four major pathways, including Bmp, Fgf, Hh, and Notch. Moreover, we identified 217 genes that were differentially expressed greater than twofold in conditional *Isl1* mutants. To date, we have confirmed six differentially expressed genes

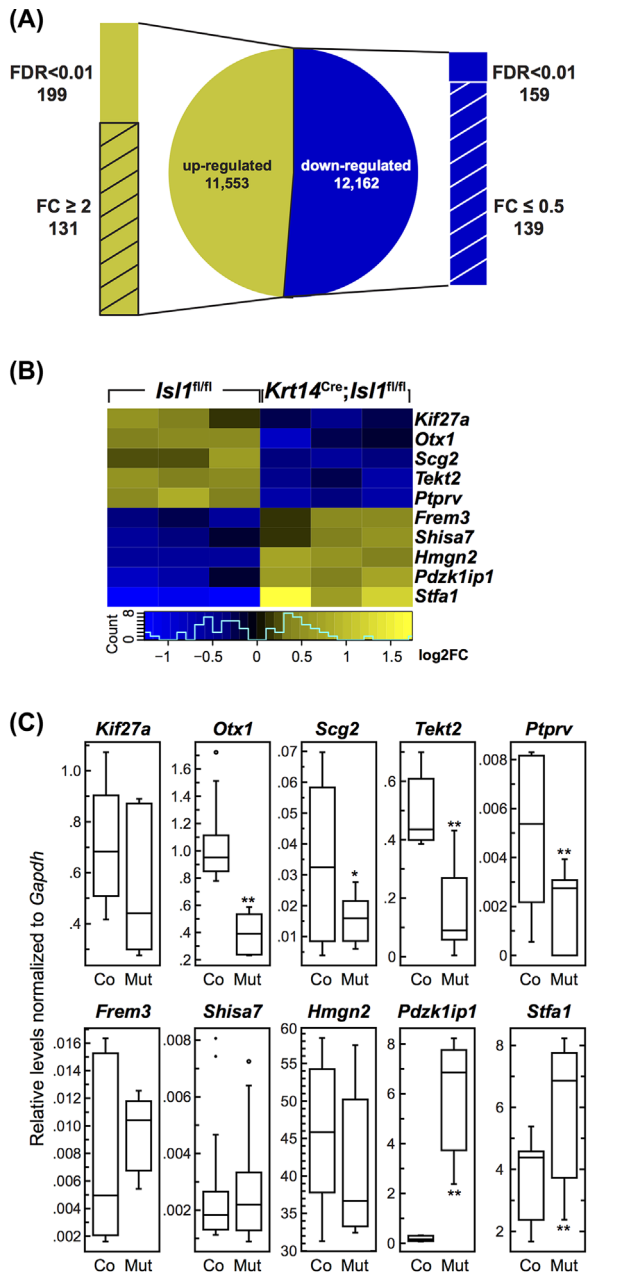

Fig. 8. Identification of differentially expressed genes between control and mutant mandibular incisors at E15.5 using RNA-Seq. (*A*) RNA-Seq analysis revealed 357 differentially regulated genes with an FDR < 0.01. From this list, 131 genes were upregulated twofold or higher (ie, $\log_2$ FC) and 139 genes were downregulated 0.5-fold or lower. (*B*) Genes identified using RNA-Seq were confirmed to be differentially expressed between developing control (Co) and mutant (Mut) incisors using qPCR. (*C*) *Kif27a* and *Stfa1* expression levels were significantly higher in mutants compared to controls, whereas *Otx2*, *Ptprv*, *Scg2*, and *Tekt2* were significantly lower in mutants. $^{*}p < 0.05$; $^{**}p < 0.01$. FDR = false discovery rate; FC = fold change; Co = control; Mut = mutant.

(ie, *Otx1*, *Scg2*, *Tekt2*, *Ptprv*, *Pdzk1ip1*, and *Stfa1*) that are regulated by ISL1 (Fig. 8*C*). We will further analyze our RNA-Seq data and Ingenuity Pathway Analysis (IPA)-generated results (Supporting Fig. S6B,C) to discover additional information regarding the downstream ISL1 targets. Together, these findings point to ISL1 as a central factor in incisor amelogenesis.

Beyond the four major signaling pathways affected, we also observed that CLDN1 was present in mutant adult liCL, where it is not normally expressed (Fig. 6*M*,*N*). Differences in expression were first observed at E17.5, when CLDN1 localization was sustained in the mutant liCL (Fig. 7*I*–*N*). CLDN1 is a component of tight junctions essential for proper cell-cell adhesion and is expressed along with other claudins during mouse incisor and molar development.[61,62] Recently, it was shown that a deficiency in CLDN16 led to defects in the tight junctions of secretory ameloblasts that led to amelogenesis imperfecta.[63] SEM analysis of *Isl1* mutant incisors revealed that labial inter-rods were disrupted near the tooth surface in the outer enamel but not near the DEJ in the inner (Fig. 3*A*–*E*), suggestive of defects in secretory ameloblasts.[64] Although differences in CLDN1 expression were not apparent on the labial side of *Isl1* mutant incisors (Fig. 6*O*,*P*), it would be interesting to determine whether similar, altered inter-rod patterns are present in *Cldn16*-deficient mice.[63]

ISL1 functions in a context-dependent manner and is important in the determination of the crown versus the root. The labial side of the mouse incisor is often considered to be the tooth crown analog, whereas the lingual side is the root analog. Enamel on the labial surface was prematurely mineralized in mutant incisors (Fig. 2*D*,*H*) likely due to premature differentiation of ameloblasts (Fig. 3*F*–*O*; Supporting Fig. S3A-H,M) and decreased proliferation of TA cells (Fig. 4*E*–*H*). SEM analysis revealed that labial enamel was altered in the mutant incisor (Fig. 3*A*–*D*^{3}) but interestingly, we did not detect any density differences with additional μCT and SEM backscatter analyses (Supporting Fig. S2E-J). On the lingual side, we noted ectopic enamel (Fig. 2*D*,*D*′,*H*,*H*′) because of the presence of ectopic ameloblasts indicated by the expression of enamel proteins such as AMEL, AMBN, AMTN, ENAM, and KLK4 (Fig. 3*F*–*O*; Supporting S3), and the density of the ectopic lingual enamel was similar to that of labial enamel (Supporting Fig. S2E). Moreover, there was an increase in proliferative cells in the liCL (Fig. 4*A*–*D*), and differential expression of numerous genes between the liCL and laCL in control and mutant mice was observed. For example, *Shh* and *Etv5* expression was upregulated in mutant liCL but downregulated in mutant laCL (Fig. 5). The seemingly opposite effects observed with epithelial *Isl1* inactivation in the liCL and laCL, specifically in proliferation and gene expression, strongly suggest context-dependent regulation of ISL1 that will be fertile ground for future studies. It will be interesting to determine whether there are changes in molar root development in *Isl1* mutant mice, as well as in three other mouse models that generate ectopic enamel and/or ameloblast-like cells from the liCL.[15,18,19]

The specific effect of epithelial *Isl1* inactivation on continuously renewing mouse incisors but not molars (Fig. 2*D*,*H*; Supporting S2A-D). We did not detect any *Isl1* expression during molar development (E14.5 to 6 weeks old). A previous report indicated slight expression of *Isl1* during molar development at E11.5 and P4.[33] These prior experiments were whole-mount in situ hybridization that showed very limited *Isl1* expression profiles on the lingual side of the developing molar at E11.5 and in the enamel-free cusp region at P4. Although it is possible that we did not analyze these specific sections in our study, it is difficult to confirm the prior report because no negative control sections were presented.[33] Regardless of the limited *Isl1* expression in molars, we conclude that molar development

was not affected by *Isl1* inactivation (Supporting Fig. S2A-D). Our results strongly support a potential role for *Isl1* in the development of anterior teeth (eg, incisors and canines), as well as in the regulation of DESCs. This hypothesis is further supported by the specific expression of *Isl1* in anterior teeth but not posterior teeth (eg, molars) in humans.[35] *Isl1* also appears to be a critical factor for maintaining labio-lingual asymmetry, as deletion of this gene leads the laCL and liCL regions to become more similar to one another.

Our RNA-Seq experiment comparing control and mutant E15.5 incisors produced an extensive list of differentially regulated genes to focus on in future studies (Fig. 8; Supporting S6). GO analysis revealed association of these genes to biological functions or components and highlighted annotation clusters showing the potential importance of protein translation, trafficking, localization, and cell signaling (Supporting Fig. S6). The relatively large presence of clusters encompassing immune response terms was not surprising, given that the dental mesenchyme at this stage houses numerous immune cells.[65]

Our data suggest that there are least three distinct molecular mechanisms for the generation of enamel: molar ameloblasts do not require *Isl1* to develop properly, laCL-generated ameloblasts do, and the absence of *Isl1* leads to liCL-generated ectopic ameloblasts and enamel. Together, our findings demonstrate that ISL1 is a central factor in patterning of proper incisor amelogenesis and that it is an upstream regulator of multiple signaling pathways and genes.

Disclosures

All authors state that they have no conflicts of interest.

Acknowledgments

This work was supported by grants from the National Institutes of Health (R35-DE026602 and R01-DE021420 to ODK, and R00-DE022059 to AHJ). AN was supported by the Université Paris Descartes – Sorbonne Paris Cité, Fondation Bettencourt-Schueller, Institut Servier, Fondation des Gueules-Cassées, Fondation Philippe, and Assistance Publique-Hôpitaux de Paris. μCT imaging work was performed in part by Sabra Djomehri in the UCSF Division of Biomaterials and Bioengineering Micro-CT Imaging Facility, supported by the Dept. of Health and Human Services/NIH S10 Shared Instrumentation Grant (S10RR026645) and the Departments of Preventive and Restorative Dental Sciences and Orofacial Sciences, School of Dentistry, UCSF. We also thank the Laurel Foundation Endowment for Craniofacial Research at the University of Washington.

Authors' roles: Study design: AHJ and ODK. Animal treatment: AN, BM, TW, KBJ, and AHJ. Histology, in situ hybridization, and immunostaining: AN, BZ, BM, MTS, TW, and AHJ. μCT: TCC. SEM: BG and AHJ. qPCR data collection and analyses: BM, MP, and AHJ; RNA-Seq analysis: PM and AHJ. Data interpretation: AN, BZ, AHJ, and ODK. Manuscript preparation: AN, BZ, AHJ, and ODK. Approval of final versions of manuscript: All authors. AHJ and ODK are responsible for the integrity of data analysis.

References

1. Jheon AH, Seidel K, Biehs B, Klein OD. From molecules to mastication: the development and evolution of teeth. Wiley Interdiscip Rev Dev Biol. 2013;2(2):165–82.
2. Harada H, Kettunen P, Jung HS, Mustonen T, Wang YA, Thesleff I. Localization of putative stem cells in dental epithelium and their association with Notch and FGF signaling. J Cell Biol. 1999;147(1):105–20.
3. Seidel K, Ahn CP, Lyons D, et al. Hedgehog signaling regulates the generation of ameloblast progenitors in the continuously growing mouse incisor. Development. 2010;137(22):3753–61.
4. Li CY, Cha W, Luder HU, et al. E-cadherin regulates the behavior and fate of epithelial stem cells and their progeny in the mouse incisor. Dev Biol. 2012;366(2):357–66.
5. Juuri E, Saito K, Ahtiainen L, et al. Sox2+ stem cells contribute to all epithelial lineages of the tooth via Sfrp5+ progenitors. Dev Cell. 2012;23(2):317–28.
6. Biehs B, Hu JK, Strauli NB, et al. BMI1 represses Ink4a/Arf and Hox genes to regulate stem cells in the rodent incisor. Nat Cell Biol. 2013;15(7):846–52.
7. Smith CE, Warshawsky H. Cellular renewal in the enamel organ and the odontoblast layer of the rat incisor as followed by radioautography using 3H-thymidine. Anat Rec. 1975;183(4):523–61.
8. Smith CE, Warshawsky H. Histological and three dimensional organization of the odontogenic organ in the lower incisor of 100 gram rats. Am J Anat. 1975;142(4):403–29.
9. Warshawsky H, Smith CE. Morphological classification of rat incisor ameloblasts. Anat Rec. 1974;179(4):423–46.
10. Bei M, Maas R. FGFs and BMP4 induce both Msx1-independent and Msx1-dependent signaling pathways in early tooth development. Development. 1998;125(21):4325–33.
11. Mitsiadis TA, Hirsinger E, Lendahl U, Goridis C. Delta-notch signaling in odontogenesis: correlation with cytodifferentiation and evidence for feedback regulation. Dev Biol. 1998;204(2):420–31.
12. Harada H, Toyono T, Toyoshima K, et al. FGF10 maintains stem cell compartment in developing mouse incisors. Development. 2002;129(6):1533–41.
13. Millar SE, Koyama E, Reddy ST, et al. Over- and ectopic expression of Wnt3 causes progressive loss of ameloblasts in postnatal mouse incisor teeth. Connect Tissue Res. 2003;44 Suppl 1:124–9.
14. Wang XP, Suomalainen M, Jorgez CJ, Matzuk MM, Werner S, Thesleff I. Follistatin regulates enamel patterning in mouse incisors by asymmetrically inhibiting BMP signaling and ameloblast differentiation. Dev Cell. 2004;7(5):719–30.
15. Wang XP, Suomalainen M, Felszeghy S, et al. An integrated gene regulatory network controls stem cell proliferation in teeth. PLoS Biol. 2007;5(6):e159.
16. Felszeghy S, Suomalainen M, Thesleff I. Notch signalling is required for the survival of epithelial stem cells in the continuously growing mouse incisor. Differentiation. 2010;80(4–5):241–8.
17. Liu F, Dangaria S, Andl T, et al. beta-Catenin initiates tooth neogenesis in adult rodent incisors. J Dent Res. 2010;89(9):909–14.
18. Klein OD, Lyons DB, Balooch G, et al. An FGF signaling loop sustains the generation of differentiated progeny from stem cells in mouse incisors. Development. 2008;135(2):377–85.
19. Kyrylkova K, Kyryachenko S, Biehs B, Klein O, Kioussi C, Leid M. BCL11B regulates epithelial proliferation and asymmetric development of the mouse mandibular incisor. PLoS One. 2012;7(5):e37670.
20. Karlsson O, Thor S, Norberg T, Ohlsson H, Edlund T. Insulin gene enhancer binding protein Isl-1 is a member of a novel class of proteins containing both a homeo- and a Cys-His domain. Nature. 1990;344(6269):879–82.
21. Pfaff SL, Mendelsohn M, Stewart CL, Edlund T, Jessell TM. Requirement for LIM homeobox gene Isl1 in motor neuron generation reveals a motor neuron-dependent step in interneuron differentiation. Cell. 1996;84(2):309–20.
22. Ericson J, Norlin S, Jessell TM, Edlund T. Integrated FGF and BMP signaling controls the progression of progenitor cell differentiation and the emergence of pattern in the embryonic anterior pituitary. Development. 1998;125(6):1005–15.
23. Hunter CS, Dixit S, Cohen T, et al. Islet alpha-, beta-, and delta-cell development is controlled by the Ldb1 coregulator, acting primarily with the islet-1 transcription factor. Diabetes. 2013;62(3):875–86.

24. Witzel HR, Jungblut B, Choe CP, Crump JG, Braun T, Dobreva G. The LIM protein Ajuba restricts the second heart field progenitor pool by regulating Isl1 activity. Dev Cell. 2012;23(1):58–70.
25. Kawakami Y, Marti M, Kawakami H, et al. Islet1-mediated activation of the beta-catenin pathway is necessary for hindlimb initiation in mice. Development. 2011;138(20):4465–73.
26. Laugwitz KL, Moretti A, Lam J, et al. Postnatal isl1+ cardioblasts enter fully differentiated cardiomyocyte lineages. Nature. 2005;433(7026):647–53.
27. Moretti A, Caron L, Nakano A, et al. Multipotent embryonic isl1+ progenitor cells lead to cardiac, smooth muscle, and endothelial cell diversification. Cell. 2006;127(6):1151–65.
28. Bu L, Jiang X, Martin-Puig S, et al. Human ISL1 heart progenitors generate diverse multipotent cardiovascular cell lineages. Nature. 2009;460(7251):113–7.
29. Cai CL, Liang X, Shi Y, et al. Isl1 identifies a cardiac progenitor population that proliferates prior to differentiation and contributes a majority of cells to the heart. Dev Cell. 2003;5(6):877–89.
30. Caputo L, Witzel HR, Kolovos P, et al. The Isl1/Ldb1 complex orchestrates genome-wide chromatin organization to instruct differentiation of multipotent cardiac progenitors. Cell Stem Cell. 2015;17(3):287–99.
31. Heikinheimo K, Kurppa KJ, Laiho A, et al. Early dental epithelial transcription factors distinguish ameloblastoma from keratocystic odontogenic tumor. J Dent Res. 2015;94(1):101–11.
32. Wang X, Shaffer JR, Zeng Z, et al. Genome-wide association scan of dental caries in the permanent dentition. BMC Oral Health. 2012;12:57.
33. Mitsiadis TA, Angeli I, James C, Lendahl U, Sharpe PT. Role of Islet1 in the patterning of murine dentition. Development. 2003;130(18):4451–60.
34. Echelard Y, Epstein DJ, St-Jacques B, et al. Sonic hedgehog, a member of a family of putative signaling molecules, is implicated in the regulation of CNS polarity. Cell. 1993;75(7):1417–30.
35. Huang Z, Hu X, Lin C, Chen S, Huang F, Zhang Y. Genome-wide analysis of gene expression in human embryonic tooth germ. J Mol Histol. 2014;45(6):609–17.
36. Dassule HR, Lewis P, Bei M, Maas R, McMahon AP. Sonic hedgehog regulates growth and morphogenesis of the tooth. Development. 2000;127(22):4775–85.
37. Pan L, Deng M, Xie X, Gan L. ISL1 and BRN3B co-regulate the differentiation of murine retinal ganglion cells. Development. 2008;135(11):1981–90.
38. Langmead B, Salzberg SL. Fast gapped-read alignment with Bowtie 2. Nat Methods. 2012;9(4):357–9.
39. Trapnell C, Pachter L, Salzberg SL. TopHat: discovering splice junctions with RNA-Seq. Bioinformatics. 2009;25(9):1105–11.
40. Flicek P, Amode MR, Barrell D, et al. Ensembl 2014. Nucleic Acids Res. 2014;42(Database issue):D749–55.
41. Anders S, Huber W. Differential expression analysis for sequence count data. Genome Biol. 2010;11(10):R106.
42. Huang da W, Sherman BT, Lempicki RA. Systematic and integrative analysis of large gene lists using DAVID bioinformatics resources. Nat Protoc. 2009;4(1):44–57.
43. Huang da W, Sherman BT, Lempicki RA. Bioinformatics enrichment tools: paths toward the comprehensive functional analysis of large gene lists. Nucleic Acids Res. 2009;37(1):1–13.
44. Roehl H, Nusslein-Volhard C. Zebrafish pea3 and erm are general targets of FGF8 signaling. Curr Biol. 2001;11(7):503–7.
45. Klein OD, Minowada G, Peterkova R, Kangas A, Yu BD, Lesot H, et al. Sprouty genes control diastema tooth development via bidirectional antagonism of epithelial-mesenchymal FGF signaling. Dev Cell. 2006;11(2):181–90.
46. Nakamura T, Hasegawa Y, Sugino K, Kogawa K, Titani K, Sugino H. Follistatin inhibits activin-induced differentiation of rat follicular granulosa cells in vitro. Biochim Biophys Acta. 1992;1135(1):103–9.
47. Matzuk MM, Lu N, Vogel H, Sellheyer K, Roop DR, Bradley A. Multiple defects and perinatal death in mice deficient in follistatin. Nature. 1995;374(6520):360–3.
48. Rodriguez-Boulan E, Nelson WJ. Morphogenesis of the polarized epithelial cell phenotype. Science. 1989;245(4919):718–25.
49. Inai T, Sengoku A, Hirose E, Iida H, Shibata Y. Differential expression of the tight junction proteins, claudin-1, claudin-4, occludin, ZO-1, and PAR3, in the ameloblasts of rat upper incisors. Anat Rec (Hoboken). 2008;291(5):577–85.
50. Bello IO, Soini Y, Slootweg PJ, Salo T. Claudins 1, 4, 5, 7 and occludin in ameloblastomas and developing human teeth. J Oral Pathol Med. 2007;36(1):48–54.
51. Morsli H, Tuorto F, Choo D, Postiglione MP, Simeone A, Wu DK. Otx1 and Otx2 activities are required for the normal development of the mouse inner ear. Development. 1999;126(11):2335–43.
52. Yoon H, Lee DJ, Kim MH, Bok J. Identification of genes concordantly expressed with Atoh1 during inner ear development. Anat Cell Biol. 2011;44(1):69–78.
53. Shyu WC, Lin SZ, Chiang MF, et al. Secretoneurin promotes neuroprotection and neuronal plasticity via the Jak2/Stat3 pathway in murine models of stroke. J Clin Invest. 2008;118(1):133–48.
54. Hao A, Novotny-Diermayr V, Bian W, et al. The LIM/homeodomain protein Islet1 recruits Janus tyrosine kinases and signal transducer and activator of transcription 3 and stimulates their activities. Mol Biol Cell. 2005;16(4):1569–83.
55. Kassi E, Papavassiliou AG. A possible role of osteocalcin in the regulation of insulin secretion: human in vivo evidence? J Endocrinol. 2008;199(2):151–3.
56. Doumont G, Martoriati A, Marine JC. PTPRV is a key mediator of p53-induced cell cycle exit. Cell Cycle. 2005;4(12):1703–5.
57. Hayashi M, Nimura K, Kashiwagi K, et al. Comparative roles of Twist-1 and Id1 in transcriptional regulation by BMP signaling. J Cell Sci. 2007;120(Pt 8):1350–7.
58. Lundberg KC, Fritz Y, Johnston A, et al. Proteomics of skin proteins in psoriasis: from discovery and verification in a mouse model to confirmation in humans. Mol Cell Proteomics. 2015;14(1):109–19.
59. Jheon AH, Prochazkova M, Meng B, et al. Inhibition of Notch signaling during mouse incisor renewal leads to enamel defects. J Bone Miner Res. 2016 Jan;31(1):152–62.
60. Harada H, Ichimori Y, Yokohama-Tamaki T, et al. Stratum intermedium lineage diverges from ameloblast lineage via Notch signaling. Biochem Biophys Res Commun. 2006;340(2):611–6.
61. Ohazama A, Sharpe PT. Expression of claudins in murine tooth development. Dev Dyn. 2007;236(1):290–4.
62. Hoshino M, Hashimoto S, Muramatsu T, Matsuki M, Ogiuchi H, Shimono M. Claudin rather than occludin is essential for differentiation in rat incisor odontoblasts. Oral Dis. 2008;14(7):606–12.
63. Bardet C, Courson F, Wu Y, et al. Claudin-16 deficiency impairs tight junction function in ameloblasts, leading to abnormal enamel formation. J Bone Miner Res. 2016 Mar;31(3):498–513.
64. Skobe Z. The secretory stage of amelogenesis in rat mandibular incisor teeth observed by scanning electron microscopy. Calcif Tissue Res. 1976;21(2):83–103.
65. Seidel K, Marangoni P, Tang C, et al. Resolving stem and progenitor cells in the adult mouse incisor through gene co-expression analysis. eLife. 2017 May 5;6. DOI:10.7554/eLife.24712.